

## Time Evolution of Density Fluctuation in the Supercritical Region. 2. Comparison of Hydrogen- and Non-hydrogen-Bonded Fluids

Daisuke Kajiya,<sup>†</sup> Keiko Nishikawa,<sup>†</sup> and Ken-ichi Saitow<sup>\*,‡</sup>

Division of Diversity Science, Graduate School of Science and Technology, Chiba University, Yayoi, Inage, Chiba 263-8522, Japan, and Material Science Center, Natural Science Center for Basic Research and Development, Hiroshima University, 1-3-1 Kagamiyama, Higashi Hiroshima 739-8526, Japan

Received: April 28, 2005; In Final Form: June 26, 2005

The time evolution of the density fluctuation of molecules is investigated by dynamic light scattering in six neat fluids in supercritical states. This study is the first to compare the dynamics of density inhomogeneity between hydrogen- and non-hydrogen-bonded fluids. Supercritical methanol and ethanol are used as hydrogen-bonded fluids, whereas four non-hydrogen-bonded fluids were used: CHF<sub>3</sub>, C<sub>2</sub>H<sub>4</sub>, CO<sub>2</sub>, and Xe. We measure the time correlation function of the density fluctuation of each fluid at the same reduced temperatures and densities and investigate the relationship between the dynamic and static density inhomogeneities of those supercritical fluids. In all cases, the profile of the time correlation function of the density fluctuation is characterized by a single-exponential function, whose decay is responsible for the dynamics characterized by hydrodynamic conditions. We obtain correlation times from the time correlation function and discuss dynamic and static inhomogeneity using the Kawasaki theory and the Landau-Placzek theory. While the correlation times in the six fluids show noncoincidence, those values agree well with each other except for the supercritical alcohols when scaled to a dimensionless parameter. Although the principle of corresponding state is observed in the non-hydrogen-bonded fluids, both the supercritical methanol and ethanol deviate from that principle. This deviation is attributed to the presence of hydrogen bonding among alcohol molecules at high temperature and low density. The average cluster size of each fluid is estimated under the same thermodynamic conditions, and it is shown that the clusters of supercritical alcohols are on average 1.5–1.7 times larger than those of the four non-hydrogen-bonded fluids. Moreover, the thermal diffusivity of each neat fluid is obtained over wide ranges of density and temperature.

### I. Introduction

The increasing use of supercritical fluids in a wide range of practical applications has motivated a number of recent attempts to understand the fundamental aspects of fluid structure. Although for decades the inhomogeneity of fluid structures around gas–liquid critical points was considered a result of density inhomogeneity,<sup>1–5</sup> recently supercritical fluid structure has been studied in connection with efficiencies of extraction and chemical reaction. For example, the solubility, rate constant, and yield of a photochemical reaction, as well as the relaxation times of electronic, vibrational, and rotational transitions, each show either an inflection, a minimum, or a maximum around the density where the inhomogeneity is greatest. Thus, it is important to study supercritical fluids with regard to density inhomogeneity, not only to increase our understanding of the natural sciences but also to improve efficiencies in the chemical industry.

In experimental studies, the measurement of light scattering has proven to be a good basis on which to investigate inhomogeneity in the condensed phase.<sup>6–8</sup> Although light scattering studies relating to supercritical fluids started in 1970

as research into the critical phenomena of the gas–liquid critical point,<sup>9–14</sup> not many studies on fluid structures have been conducted. That is, the Rayleigh scattering intensity<sup>9–12</sup> or the Rayleigh line width<sup>12,13</sup> was measured under restricted experimental conditions, e.g., along the critical isochore, where the reduced density  $\rho_r = \rho/\rho_c$  is 1.0, and very near the gas–liquid critical temperature,  $1.000005 \leq T_r = T/T_c \leq 1.001$ . Under these conditions, correlation lengths of supercritical CO<sub>2</sub> were obtained from the former measurement as a static structure.<sup>9–11</sup> As for the dynamic structure obtained by the latter, the spectra were measured in the *frequency domain*, and rates of density fluctuation and transport coefficients were discussed for supercritical CO<sub>2</sub>,<sup>13</sup> Xe,<sup>13</sup> and SF<sub>6</sub>.<sup>12,13</sup> Recently, the dynamic structure has been investigated in the *time domain* using dynamic light scattering (DLS). This is a powerful method to investigate the time profile of density fluctuation, because the DLS experiment allows us to obtain the *time evolution* of molecules dispersed in the fluid by measuring the time correlation function. Thus, the dynamics of density fluctuation was discussed using the results of DLS measurement at density and temperature ranges extending to  $\rho_r = 0.4–2.0$  and  $T_r = 1.06$ , respectively.<sup>14–17</sup> In such a thermodynamic condition, the “critical slowing down” of diffusing molecules was observed, and a time-constant map of the critical slowing down was produced as a contour curve on phase diagrams.<sup>16</sup> The structures of the supercritical fluids observed by diffusive motion were discussed in relation to the local structures of the same fluid observed by not only

\* Corresponding author. E-mail: [saitow@hiroshima-u.ac.jp](mailto:saitow@hiroshima-u.ac.jp).

<sup>†</sup> Division of Diversity Science, Graduate School of Science and Technology, Chiba University, Yayoi, Inage, Chiba 263-8522, Japan.

<sup>‡</sup> Material Science Center, Natural Science Center for Basic Research and Development, Hiroshima University, 1-3-1 Kagamiyama, Higashi Hiroshima 739-8526, Japan.

**TABLE 1: Molecular Properties and Critical Constants**

molecule	radius (nm) <sup>a,b</sup>	volume ( $\times 10^3 \text{ nm}^3$ ) <sup>a,b</sup>	structure	polarity <sup>c</sup>	hydrogen bonding	$T_c$ (K)	$P_c$ (MPa)	$\rho_c$ ( $\text{g cm}^{-3}$ )
CH <sub>3</sub> OH	0.236	55.1	sym top	1.70 D <sup>d</sup>	O	512.6 <sup>g</sup>	8.104 <sup>g</sup>	0.276 <sup>g</sup>
C <sub>2</sub> H <sub>5</sub> OH	0.258	71.9	chain	1.69 D <sup>d</sup>	O	516.3 <sup>h</sup>	6.379 <sup>h</sup>	0.276 <sup>h</sup>
Xe	0.216	42.2	spherical		X	289.73 <sup>i</sup>	5.84 <sup>i</sup>	1.1 <sup>i</sup>
CHF <sub>3</sub>	0.214	41.1	sym top	1.65 D <sup>d</sup>	X	299.06 <sup>j</sup>	4.836 <sup>j</sup>	0.525 <sup>j</sup>
C <sub>2</sub> H <sub>4</sub>	0.210	38.8	plane	-4 DA ( $Q_{xx}$ ) <sup>e</sup> 2 DA ( $Q_{yy}=Q_{zz}$ ) <sup>e</sup>	X	282.35 <sup>k</sup>	5.042 <sup>k</sup>	0.214 <sup>k</sup>
CO <sub>2</sub>	0.201	34.0	linear	-20 DA ( $Q_{xx}$ ) <sup>f</sup> -15 DA ( $Q_{yy}=Q_{zz}$ ) <sup>f</sup>	X	304.13 <sup>l</sup>	7.377 <sup>l</sup>	0.468 <sup>l</sup>

<sup>a</sup> Data taken from ref 24. <sup>b</sup> Each molecular radius and volume are given by the van der Waals radius and volume, respectively. Their values were measured by XRD measurements from ref 24. <sup>c</sup> The units of dipole moment (D) and quadrupole moments (DA) in the table are debye and debye angstrom, respectively. The value of the quadrupole moment is represented by a tensor element in each principal axis. <sup>d</sup> Data taken from ref 25. <sup>e</sup> Data taken from ref 26. <sup>f</sup> Data taken from ref 27. <sup>g</sup> Data taken from ref 28. <sup>h</sup> Data taken from ref 29. <sup>i</sup> Data taken from ref 30. <sup>j</sup> Data taken from ref 31. <sup>k</sup> Data taken from ref 32. <sup>l</sup> Data taken from ref 33.

vibrational<sup>18–21</sup> and rotational motions<sup>18,22,23</sup> but also the fabrication of advanced nanomaterials.<sup>24</sup>

In our previous study (Part 1), several non-hydrogen-bonded molecules were investigated by DLS: supercritical CHF<sub>3</sub>, Xe, C<sub>2</sub>H<sub>4</sub>, and CO<sub>2</sub> were investigated at the same density and reduced temperature ranges, i.e.,  $T_r = 1.001–1.06$  and  $\rho_r = 0.4–2.0$ .<sup>17</sup> These molecules share similar sizes, although their molecular properties differ completely; e.g., polar (CHF<sub>3</sub>), nonpolar (Xe), and nondipolar molecules (C<sub>2</sub>H<sub>4</sub> and CO<sub>2</sub>) have symmetric top, spherical, planar, and linear shapes, respectively. Under these conditions, the dynamic and static density fluctuations were studied. The following insights were obtained: (i) viscosity is the main contributor to the time evolution of density fluctuation, (ii) the dimensionless parameter describing inhomogeneity is a common value among molecules, despite the different molecular properties, and (iii) the Kawasaki theory and the Landau-Placzek theory are confirmed to be applicable to polar, nonpolar, and nondipolar fluids in wide temperature and density ranges.

These new insights obtained from our previous work have motivated us to extend the study of the time evolution of density fluctuation to hydrogen-bonded fluids and to investigate how these fluids behave under supercritical conditions. By constructing a DLS system, which allows us to measure the time correlation function at a difficult condition of temperature  $> 500$  K and pressure of 30 MPa, we can measure the time correlation functions of density fluctuations of hydrogen-bonded fluids and compare the resultant data against those for non-hydrogen-bonded fluids. Here we show, for the first time, the time evolutions of the density fluctuations of supercritical methanol (CH<sub>3</sub>OH) and ethanol (C<sub>2</sub>H<sub>5</sub>OH). As a result, it was found that the dynamic and static density inhomogeneities of both alcohols deviate significantly from those of non-hydrogen-bonded fluids even in the same thermodynamic conditions. The differences between the hydrogen-bonded and non-hydrogen-bonded fluids are evaluated and discussed.

## II. Experimental Section

The DLS instrument used in the present study has been described elsewhere.<sup>15–17</sup> The light source was an argon ion laser operating at a single line of 488 nm at a power of 100 mW. The scattering light was collected by an optical fiber attached to a goniometer and was detected with a photomultiplier tube through the use of a photon-counting method. The counted photons were processed via a digital multiple- $\tau$  photon correlator (ALV 5000E). Data of sufficient quality were collected when the scattering angles were between 20° and 150°.

An optical cell for hydrogen-bonded fluids was designed to withstand both high pressure (40 MPa) and high temperature

(650 K) conditions and has been described in detail.<sup>25</sup> The pressure was adjusted by an HPLC pump, and fluctuations in pressure were suppressed to within  $\pm 0.01$  MPa during the measurement. A pressure gauge was calibrated by the critical point of supercritical CO<sub>2</sub>. Thus, the accuracy of pressure in the present study was within  $\pm 0.01$  MPa. The temperature was controlled by a set of heaters, a PID controller, and a thermocouple. The point of the thermocouple was positioned near the focal point of the excitation laser. The reference temperature of the thermocouple was calibrated carefully by a cold junction of ice water to an accuracy of  $\pm 0.01$  K. Thus, the temperature fluctuation was accomplished to be within  $\pm 0.1$  K at 500 K. On the other hand, the optical cell for non-hydrogen-bonded fluids was a Pyrex tube with a special smooth surface; it has been described in detail.<sup>15–17</sup> The pressure and temperature of the fluid were adjusted by an injector and by circulating water, respectively. Fluctuations in pressure and temperature during the measurement were carefully adjusted to within a deviation of  $\pm 0.03\%$ . In the present study, the accuracies of temperature and pressure were  $\pm 0.1$  K and  $\pm 0.01$  MPa, respectively.

In DLS experiments, a light intensity autocorrelation function is measured by a digital photon correlator. This function,  $g^{(2)}(t)$ , is described by the use of an electric field autocorrelation function  $g^{(1)}(t)$  as follows:<sup>6,7</sup> where  $\beta$  is the coherence factor.

$$g^{(2)}(t) = 1 + \beta |g^{(1)}(t)|^2 \quad (1)$$

By taking  $\sqrt{g^{(2)}(t)-1}$ ,  $g^{(1)}(t)$  is obtained. In the present study, all data are measured at the wave vector of  $k = |\mathbf{k}| = 4\pi n \sin(\theta/2) \cong 1.0 \times 10^{-2} \text{ nm}^{-1}$ , whose scale corresponds to a mesoscopic region in real space. The electric field correlation function here is ascribed to the time correlation of the density fluctuation.<sup>15–17</sup> This function indicates the time evolution in a mesoscopic volume, where numerous molecules are inhomogeneously dispersed.

We measured the time correlation functions of the density fluctuations of supercritical CH<sub>3</sub>OH, C<sub>2</sub>H<sub>5</sub>OH, Xe, CHF<sub>3</sub>, C<sub>2</sub>H<sub>4</sub>, and CO<sub>2</sub>, whose molecular properties<sup>26–29</sup> and critical constants<sup>30–35</sup> are listed in Table 1. The data were collected in the density range of  $0.4 \leq \rho_r \leq 1.6$  at four isotherms:  $T_r = 1.01, 1.02, 1.04,$  and  $1.06$ . To accomplish these common reduced densities and temperatures, the DLS measurements of supercritical CH<sub>3</sub>OH and C<sub>2</sub>H<sub>5</sub>OH were performed at a temperature range of 518–547 K and a pressure range of 6–13 MPa. The chemical purities of the samples were commercially guaranteed to be  $> 99.5\%$ . As for liquid CH<sub>3</sub>OH and C<sub>2</sub>H<sub>5</sub>OH, the samples were purified using molecular sieves to remove subtle water as an impurity. To increase optical purity, all fluids were filtered through a PTFE membrane filter with 0.1  $\mu\text{m}$  pores.

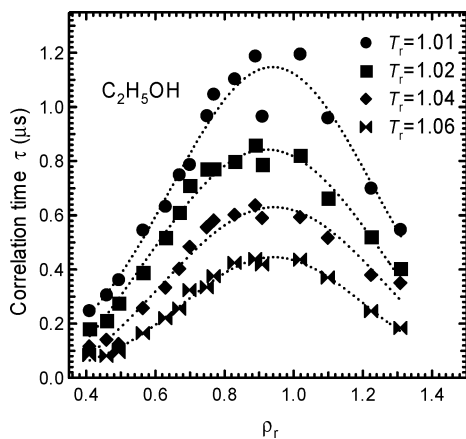


**Figure 1.** Correlation time of the density fluctuation of supercritical ethanol as a function of density at four isotherms.

### III. Results

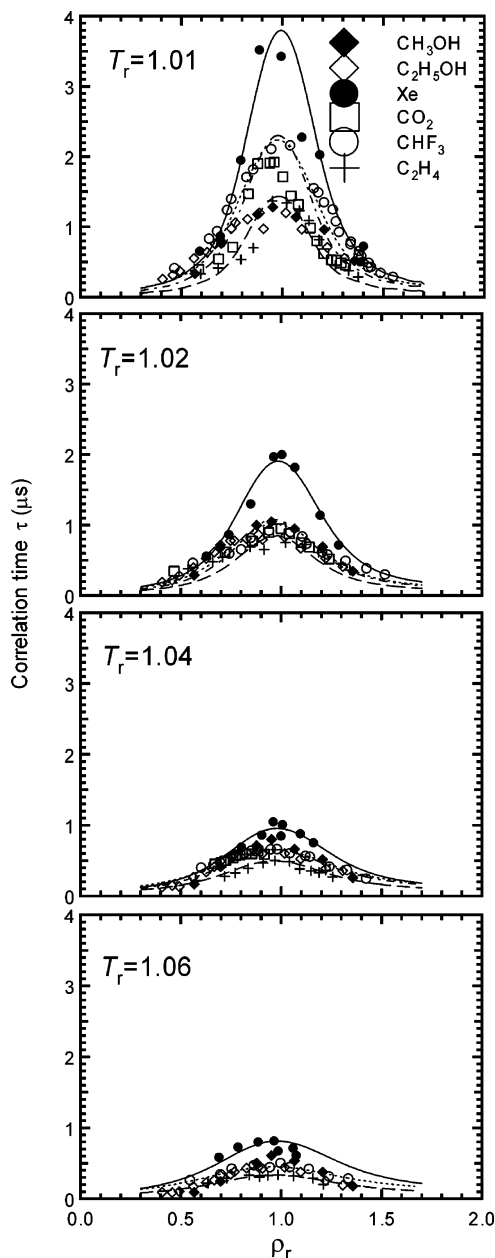
All time correlation functions measured in the present study were well analyzed by a single-exponential function, whose decay was responsible for the dynamics characterized by hydrodynamic theory.<sup>36,37</sup> In this condition, the correlation times  $\tau$  are obtained from the time correlation functions of density fluctuation in the form of  $\exp(-t/\tau)$ . As a typical example, the correlation times of supercritical  $C_2H_5OH$  are shown in Figure 1 as density dependences at several temperatures. The temperature and density change the values of the correlation times, which increase as the thermodynamic states approach the critical point. The value of the correlation time becomes considerable at around  $\rho_r = 1.0$  and  $T_r = 1.0$ . This means that the time evolution of the density fluctuation slows in the vicinity of  $\rho_r = 1.0$  and  $T_r = 1.0$ . This observation corresponds to the “critical slowing down”, a feature observed in all neat supercritical fluids.

Figure 2 shows the correlation times of all of the measured fluids at the four isotherms. The differences in the values of these fluids are observed at all measured temperatures. The correlation time for Xe is significantly greater than those of the other fluids, whereas the correlation times of the supercritical alcohols are nearly equal to those of the other fluids. Figure 3a shows the temperature dependence of each fluid’s correlation time measured at  $\rho_r = 1.0$ . All of the values decline as the temperature moves away from critical. To compare the differences among dynamic structures from molecule to molecule, we obtained the following ratio of correlation times at  $\rho_r = 1.0$  and  $T_r = 1.02$ :  $\tau(CH_3OH):\tau(C_2H_5OH):\tau(CHF_3):\tau(C_2H_4):\tau(CO_2):\tau(Xe) = 1.5:1.1:1.5:1.0:1.5:2.5$ . The higher the ratio of correlation time, the slower the time evolution of density fluctuation. Thus, this is for the first time that the time evolutions of supercritical alcohols can be compared against those of typical non-hydrogen-bonded fluids under supercritical conditions at the same thermodynamic conditions.

### IV. Discussion

We have examined the relationships among correlation time, temperature, and viscosity to investigate the contributions of each fluid to density fluctuation dynamics, since the correlation time is governed by the dynamics of the Brownian motion of molecules in viscous fluid.<sup>6,7</sup> According to the Kawasaki theory and the Landau-Placzek theory, correlation time is described as follows:<sup>38,39</sup> where  $\tau$  is the correlation time,  $k$  the scattering

$$(1/\tau k^2) = D_T = (\lambda/\rho C_p) = (k_B T/6\pi\eta\xi)(\lambda/\lambda_c) \quad (2)$$



**Figure 2.** All correlation times measured in the supercritical regions. The data show the times of supercritical  $CH_3OH$ ,  $C_2H_5OH$ , Xe,  $CHF_3$ ,  $CO_2$ , and  $C_2H_4$  as functions of densities at four isotherms.

vector,  $D_t$  the thermal diffusivity,  $\lambda$  the thermal conductivity,  $\rho$  the density,  $C_p$  the specific heat capacity at constant pressure,  $k_B$  the Boltzmann constant,  $T$  the temperature,  $\eta$  the viscosity,  $\xi$  the correlation length, and  $\lambda_c$  the critical part of thermal conductivity. Here a part of eq 2 is rewritten as follows: where

$$(k_B T/6\pi\eta\xi)(\lambda/\lambda_c) = (k_B T/6\pi\eta R_h) \quad (3)$$

$R_h$  corresponds to the average hydrodynamic radius of clusters in supercritical fluids. Note that the cluster in the current study does not mean a rigid cluster such as metal cluster but a molecular aggregate. Using eqs 2 and 3, we investigated the fluid dependence of the correlation time by using the values of viscosity ( $CH_3OH$ ,<sup>40</sup>  $C_2H_5OH$ ,<sup>41</sup>  $CHF_3$ ,<sup>42</sup>  $CO_2$ ,<sup>43</sup>  $C_2H_4$ ,<sup>44</sup> Xe<sup>45</sup>), temperature, and density and discuss the use of a static parameter ( $R_h$ ). Published viscosity data were utilized for the present study.<sup>46</sup> Figure 3b shows the  $R_h$  values of four fluids at density  $\rho_r = 1.0$  as a function of temperature. The  $R_h$  values become

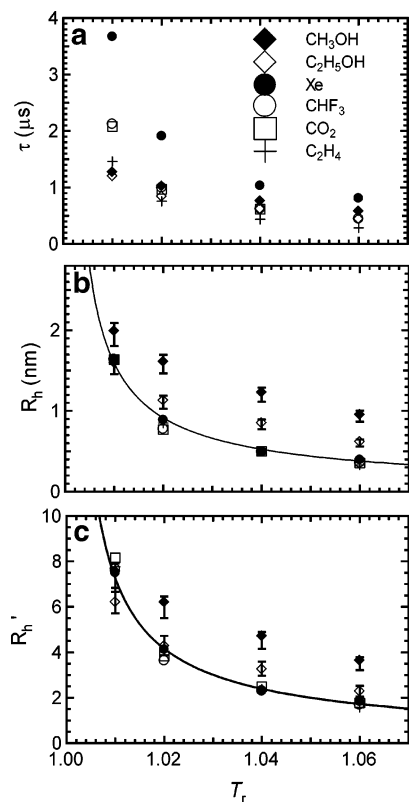


**Figure 3.** Temperature dependences of (a) correlation times, (b) hydrodynamic radii of clusters, and (c) reduced hydrodynamic radii of clusters of supercritical CH<sub>3</sub>OH, C<sub>2</sub>H<sub>5</sub>OH, Xe, CHF<sub>3</sub>, CO<sub>2</sub>, and C<sub>2</sub>H<sub>4</sub>. The data are obtained at the reduced density  $\rho_r = \rho/\rho_c = 1.0$ .

almost the same in the four non-hydrogen-bonded fluids at all reduced temperatures and densities in the present ranges. On the other hand, the  $R_h$  values of supercritical CH<sub>3</sub>OH and C<sub>2</sub>H<sub>5</sub>OH differ completely from those of the non-hydrogen-bonded fluids. These results indicate that, although the time evolution of density fluctuation of non-hydrogen-bonded fluids shows significant molecular dependence, such dependence disappears by scaling the dynamic parameter to the static parameter by the use of viscosity. For the hydrogen-bonded fluids, however, it was found that the viscosity does not compensate for the molecular dependence.

Next, we introduce another parameter—the reduced hydrodynamic radius  $R'_h$ . Since a hydrodynamic radius is reduced by dividing  $R_h$  by the van der Waals radius,  $R'_h$  results in a dimensionless parameter. As described above, the value of  $R_h$  is the average radius of clusters in the neat supercritical fluids. Since this dimensionless parameter is the cluster size divided by the molecular size, the resulting value,  $R'_h$ , tells us how many molecules are in the cluster. That is, the larger the  $R'_h$ , the greater the number of molecules. Figure 3c shows the  $R'_h$  values of all fluids as a function of temperature. It can be seen that these values agree well among non-hydrogen-bonded fluids. According to the principle of corresponding state, it is known that the universality among different fluids appears around the critical point and that the molecular properties disappear around that point by reducing the physical value to a dimensionless parameter, despite the significant differences in polarity, shape, and structure of molecules.<sup>1</sup> In the previous paper, this coincidence among non-hydrogen-bonded fluids was attributed to the principle of corresponding states.<sup>17</sup> This result is natural from the standpoint of critical phenomena.

Note that the supercritical alcohols differ significantly from the non-hydrogen-bonded fluids, as shown in Figure 3c. The

values of  $R'_h$  of supercritical CH<sub>3</sub>OH and C<sub>2</sub>H<sub>5</sub>OH are larger than those of the non-hydrogen-bonded fluids. That is, the clusters of the hydrogen-bonded fluids contain more molecules than those of the non-hydrogen-bonded fluids at the same reduced density and temperature. Similar results were observed in two previous studies. First, the reduced correlation length of supercritical water was found to be greater than those of typical fluids.<sup>47</sup> From eq 3, the reduced correlation length  $\xi'$  is combined directly with the reduced hydrodynamic radius,  $\xi' = \lambda/\lambda_c R'_h$ , where  $\lambda/\lambda_c$  is constant. The larger  $\xi'$  is attributed to hydrogen bonding at the supercritical states. Second, it was observed by Raman spectral analysis that the local density of supercritical CH<sub>3</sub>OH is 1.7 times greater than those of typical fluids, such as C<sub>2</sub>H<sub>6</sub> and CHF<sub>3</sub>, at  $T_r = 1.02$ .<sup>19</sup> This greater local density was attributed to the strong intermolecular interactions resulting from hydrogen bonding in supercritical CH<sub>3</sub>OH. In addition, it is noted that the  $R'_h$  value of supercritical CH<sub>3</sub>OH in the current study is 1.5–1.7 times greater than those of C<sub>2</sub>H<sub>4</sub> and CHF<sub>3</sub> at  $\rho_r = 1.0$  and  $T_r = 1.02$ . Accordingly, it is shown that the larger cluster size of the supercritical CH<sub>3</sub>OH gives its greater local density. As a study on the hydrogen bonding among CH<sub>3</sub>-OH molecules, the NMR measurement was performed at the supercritical state.<sup>48</sup> From that study it can be seen that the hydrogen bonding of supercritical CH<sub>3</sub>OH exists at  $T_r = 1.02$  at  $\rho_r = 1.008$ , although the degree of bonding is three times smaller than that of liquid CH<sub>3</sub>OH at room temperature. On the basis of these experimental results, it can be considered that the hydrogen bonding among CH<sub>3</sub>OH and/or C<sub>2</sub>H<sub>5</sub>OH molecules gives a greater  $R'_h$  value than those of non-hydrogen-bonded fluids and that larger clusters are formed in the supercritical alcohols than in the other fluids at the same reduced temperature and density.

Another fruitful information seen from Figure 3c is that the  $R'_h$  value of CH<sub>3</sub>OH is larger than that of C<sub>2</sub>H<sub>5</sub>OH. This means that the hydrogen bonding of supercritical CH<sub>3</sub>OH is stronger than that of supercritical C<sub>2</sub>H<sub>5</sub>OH. It is shown that the average size of the cluster of supercritical CH<sub>3</sub>OH is larger than that of supercritical C<sub>2</sub>H<sub>5</sub>OH and that the number of molecules formed in the cluster is greater in the supercritical CH<sub>3</sub>OH at the same density and temperature. A similar result was observed in an NMR study of supercritical CH<sub>3</sub>OH and C<sub>2</sub>H<sub>5</sub>OH.<sup>49</sup> In that report, the hydrogen bondings of these two fluids were evaluated, and the extent of hydrogen bond of supercritical CH<sub>3</sub>OH is larger than that of supercritical C<sub>2</sub>H<sub>5</sub>OH at the same thermodynamic conditions.

In summary, the average cluster sizes in six neat fluids were investigated at the same reduced temperatures and reduced densities by the dynamic light scattering method. A difference of the cluster size,  $R'_h$ , was found between the non-hydrogen-bonded fluids and the hydrogen-bonded fluids. One thinks that to investigate the cluster size of these six fluids by a theoretical method, e.g., molecular dynamics simulation, would help to further the understanding of cluster size in various supercritical fluids. We hope that such a study will appear in the near future.

Finally, we report the thermal diffusivities ( $D_t$ ) of all the fluids. As described in eq 2, the values of  $D_t$  are obtained from the correlation time as a function of the scattering vector; the slope in Figure 4 gives the thermal diffusivity.<sup>50</sup> By performing these analyses at each density and temperature, we obtain the  $D_t$  of both the hydrogen-bonded and the non-hydrogen-bonded fluids over wide ranges of reduced temperature and density. To the best of our knowledge, there were a few reports on the  $D_t$  values of these fluids. That is, supercritical CHF<sub>3</sub><sup>56</sup> and Xe<sup>57</sup> were investigated only along the critical isochore, although the

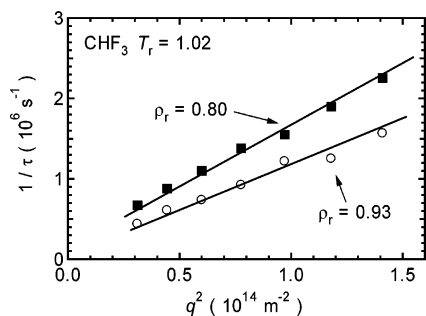


**Figure 4.** Correlation times of supercritical CHF<sub>3</sub> as a function of scattering vector. The slopes give the thermal diffusivities.

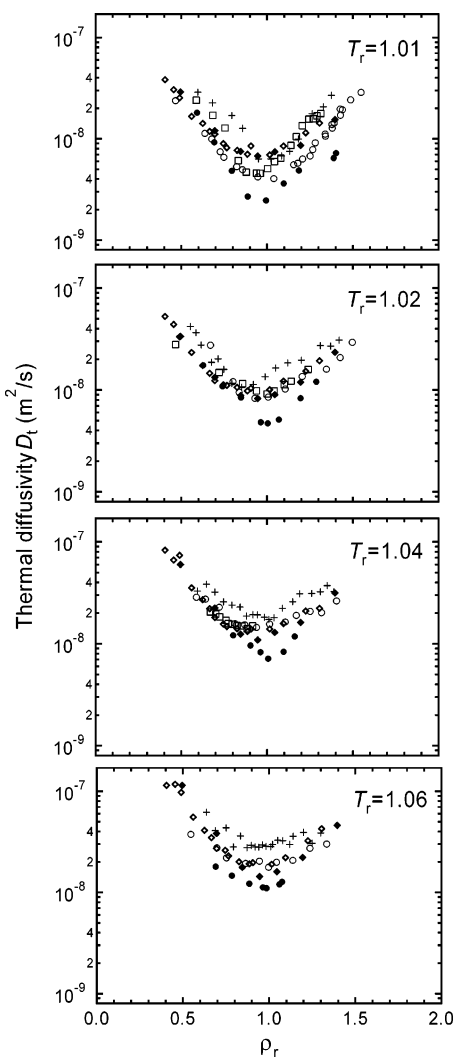


**Figure 5.** Thermal diffusivities of supercritical CH<sub>3</sub>OH (◆), C<sub>2</sub>H<sub>5</sub>OH (◇), Xe(●), CHF<sub>3</sub>(○), CO<sub>2</sub>(□), and C<sub>2</sub>H<sub>4</sub>(+) as functions of densities at four isotherms.

$D_t$  of supercritical CO<sub>2</sub> was investigated in various thermodynamic conditions,<sup>58</sup> that of supercritical C<sub>2</sub>H<sub>4</sub><sup>15</sup> was given by our previous data, and those of CH<sub>3</sub>OH and C<sub>2</sub>H<sub>5</sub>OH were reported not for the neat fluids but by the data on supercritical solutions of analyses of solute molecules.<sup>59</sup> Figure 5 shows the  $D_t$  of supercritical CH<sub>3</sub>OH, C<sub>2</sub>H<sub>5</sub>OH, Xe, C<sub>2</sub>H<sub>4</sub>, CO<sub>2</sub>, and CHF<sub>3</sub>, while the values are listed as tables in the Supporting Information on the website.<sup>60</sup> All of these fluids show minimum values at around  $\rho_r = 1.0$ , where the differences in  $D_t$  among fluids become significant. These values of  $D_t$  can be utilized to obtain specific heat capacities and thermal conductivities shown in eq 2, across wide density and temperature ranges of these six

supercritical fluids. In particular, the data on the supercritical alcohols will be important not only for natural science but also for the chemical industry. This is because information on the fluid properties of supercritical alcohols has been lacking even though supercritical alcohols are frequently used in the chemical industry—e.g., for the decomposition of plastic bottles made of PET (poly(ethylene terephthalate)) by supercritical CH<sub>3</sub>OH.

## V. Concluding Remarks

The dynamics of fluctuations in the density of supercritical CH<sub>3</sub>OH, C<sub>2</sub>H<sub>5</sub>OH, CHF<sub>3</sub>, C<sub>2</sub>H<sub>4</sub>, CO<sub>2</sub>, and Xe were studied by observing the time evolution of molecules in supercritical states from measurements of dynamic light scattering. The obtained time correlation functions were analyzed on the basis of the Kawasaki theory and the Landau-Placzek theory. The molecular dependences of dynamic and static fluctuations were studied under conditions relatively far from the gas–liquid critical points of these four fluids.

The time evolution of molecules inhomogeneously dispersed is characterized by a single-exponential function in all thermodynamic states and for all fluids. It was shown that hydrogen-bonded and non-hydrogen-bonded fluids are characterized by hydrodynamic theory within the present ranges of experimental conditions.

The correlation times of density fluctuation were not the same among the fluids but depended significantly on the type of molecules in each fluid. When the obtained dynamic parameters were scaled to the dimensionless parameter of reduced hydrodynamic radius, the molecular dependence disappeared completely among non-hydrogen-bonded fluids. On the other hand, the supercritical alcohols differed from the non-hydrogen-bonded fluids in that their clusters were, on average, larger than those of the non-hydrogen-bonded fluids at the same thermodynamic condition of supercritical states. We attribute this difference to the fact that hydrogen bonding generates clusters having much larger numbers of molecules than is the case in non-hydrogen-bonded fluids. In addition, it was elucidated that the hydrogen bonding of supercritical CH<sub>3</sub>OH is stronger than that of C<sub>2</sub>H<sub>5</sub>OH at the same reduced density and temperature.

The thermal diffusivities of all six supercritical fluids were estimated by measuring the correlation time as a function of the scattering vector, which was calibrated by the measured refractive index. The diffusivity values were, for the first time, compared with each other across wide temperature and density ranges.

**Acknowledgment.** This work was partially supported by a Grant-in-Aid for Scientific Research from the Ministry of Education, Science, and Culture, Japan. K.S. thanks the Collaboration Research Foundation for a Grant for Young Researchers at the Graduate School of Science and Technology of Chiba University and the Sumitomo Foundation Award for Young Researchers. These grants helped us to develop the instrument used in this study.

**Supporting Information Available:** Six tables showing the data of Figure 5. This material is available free of charge via the Internet at <http://pubs.acs.org>.

## References and Notes

- (1) Stanley, H. E. *Introduction to Phase Transitions and Critical Phenomena*; Oxford University Press: New York, 1971.
- (2) Greer, S. C.; Moldover, M. R. *Annu. Rev. Phys. Chem.* **1981**, *32*, 233.

- (3) Sengers, J. V.; Sengers, J. M. H. L. *Annu. Rev. Phys. Chem.* **1986**, 37, 189.
- (4) Kajimoto, O. *Chem. Rev.* **1999**, 99, 355.
- (5) Tucker, S. C. *Chem. Rev.* **1999**, 99, 391.
- (6) Berne, B. J.; Pecora, R. *Dynamic Light Scattering*; Wiley-International: New York, 1976.
- (7) Chu, B. *Laser Light Scattering: Basic Principles and Practice*; Academic Press: Boston, 1991.
- (8) Mountain, R. D. *Rev. Mod. Phys.* **1966**, 38, 205.
- (9) Lunacek, J. H.; Cannell, D. S. *Phys. Rev. Lett.* **1971**, 27, 841.
- (10) Maccabee, B. S.; White, J. A. *Phys. Lett.* **1971**, 35A, 187.
- (11) White, J. A.; Maccabee, B. S. *Phys. Rev. Lett.* **1971**, 26, 1468.
- (12) Cannel, D. S. *Phys. Rev. A* **1975**, 12, 225.
- (13) Swinney, H. L.; Henry, D. L. *Phys. Rev.* **1973**, 8, 2586 and references therein.
- (14) Letaief, A.; Tufeu, R.; Garrabos, Y.; Neindre, B. L. *J. Chem. Phys.* **1986**, 84, 921.
- (15) Saitow, K.; Ochiai, H.; Kato, T.; Nishikawa, K. *J. Chem. Phys.* **2002**, 116, 4985.
- (16) Saitow, K.; Kajiya, D.; Nishikawa, K. *J. Am. Chem. Soc.* **2004**, 126, 422.
- (17) Saitow, K.; Kajiya, D.; Nishikawa, K. *J. Phys. Chem. A* **2005**, 109, 83.
- (18) Nakayama, H.; Saitow, K.; Sakashita, M.; Ishii, K.; Nishikawa, K. *Chem. Phys. Lett.* **2000**, 320, 323.
- (19) Saitow, K.; Sasaki, J. *J. Chem. Phys.* **2005**, 122, 104502 1–12.
- (20) Saitow, K.; Nakayama, H.; Ishii, K.; Nishikawa, K. *J. Phys. Chem. A* **2004**, 108, 5770.
- (21) Saitow, K.; Otake, H.; Nakayama, H.; Ishii, K.; Nishikawa, K. *Chem. Phys. Lett.* **2003**, 368, 209.
- (22) Saitow, K.; Ohtake, H.; Sarukura, N.; Nishikawa, K. *Chem. Phys. Lett.* **2001**, 341, 86.
- (23) Saitow, K.; Nishikawa, K.; Ohtake, H.; Sarukura, N.; Miyagi, H.; Shimokawa, Y.; Matsuo, Y.; Tominaga, K. *Rev. Sci. Instrum.* **2000**, 71, 4061.
- (24) Saitow, K. *J. Phys. Chem. B* **2005**, 109, 3731.
- (25) Otake, K.; Abe, M.; Nishikawa, K.; Saitow, K. *Rev. Sci. Instrum.*, submitted for publication, 2005.
- (26) Edward, J. T. *J. Chem. Educ.* **1970**, 47, 261.
- (27) Townee C. H.; Schawlow, A. L. *Microwave Spectroscopy*; Dover: New York, 1975.
- (28) Gray, C. G.; Gubbins, K. E.; Dagg, I. R.; Read, L. A. A. *Chem. Phys. Lett.* **1980**, 73, 278.
- (29) Glaser, R.; Wu, Z.; Lewis, M. J. *Mol. Struct.* **2000**, 556, 131.
- (30) de Reuck, K. M. *Methanol, International Thermodynamic Tables of the Fluid State*; Blackwell Scientific Publications, 1993; Vol. 12.
- (31) Bhattacharyya, D.; Thodos, G. *Can. J. Chem. Eng.* **1965**, 43, 150.
- (32) McCarty, R. D. *Corrections for the Thermophysical Properties of Xenon*; NIST: Boulder, CO, 1989.
- (33) Aizpiri, A. G.; Rey, J.; Davila, J.; Rubio, R. G.; Zollweg, J. A.; Streett, B. J. *Chem. Phys.* **1991**, 95, 3351.
- (34) Smulkara, J.; Span, R.; Wanger, W. J. *Phys. Chem. Ref. Data* **2000**, 29, 1053.
- (35) Span, R.; Wagner, W. J. *Phys. Chem. Ref. Data* **1996**, 25, 1509.
- (36) Kawasaki, K. *Ann. Phys.* **1970**, 61, 1.
- (37) Kawasaki, K. *Phys. Rev. A* **1970**, 1, 1750.
- (38) Sengers, J. V.; Keyes, P. H. *Phys. Rev. Lett.* **1971**, 26, 70 and references therein.
- (39) Maccabee, B. S.; White, J. A. *Phys. Rev. Lett.* **1971**, 27, 495 and references therein.
- (40) Stephan, K.; Lucas, K. *Viscosity of Dense Fluids*; Plenum Press: New York, 1979.
- (41) Ho, C. Y. *Properties of Inorganic and Organic Fluids*; Hemisphere Publishing Corp.: New York, 1988.
- (42) Yokoyama, C.; Takahashi, M. *Int. J. Thermophys.* **1997**, 18, 1369.
- (43) Iwasaki, H.; Takahashi, M. *J. Chem. Phys.* **1981**, 74, 1930.
- (44) Iwasaki, H.; Takahashi, M. In *Proceedings of the 4th International Conference on High Pressure*; Kyoto 523 1974.
- (45) Stumpt, H. J.; Collings, A. F.; Pings, C. J. *J. Chem. Phys.* **1974**, 60, 3109.
- (46) By reviewing the various reports for viscosities of supercritical fluids, it is shown that the viscosity is almost independent of temperature but is dependent significantly on density. In addition, the value of viscosity does not show critical anomalies in the temperature of  $T_r > 1.01$ . By interpolating reported viscosities (refs 40–45) of supercritical fluids on reproduced figures, the viscosities used in the present study were obtained carefully. Thus, we can obtain good correlations between the viscosity and density of the supercritical alcohols as well as non-hydrogen-bonded fluids and were able to estimate suitable values of viscosities of the supercritical fluids used in the study.
- (47) Arai, A. A.; Morita, T.; Nishikawa, K. *J. Chem. Phys.* **2003**, 119, 1502.
- (48) Asahi, N.; Nakamura, Y. *J. Chem. Phys.* **1998**, 109, 9879.
- (49) Hoffmann, M. M.; Conradi, A. S. *J. Phys. Chem. B* **1998**, 102, 263.
- (50) Correlation times were obtained at the scattering vectors,  $k = 4\pi n \sin(\theta/2) / \lambda$ , whose values are calibrated from the other measurements (ref 51). That is, we measured the refractive indices,  $n$ , of fluids at each density and temperature by a laser beam displacement method (ref 52). The indices were obtained carefully at the wavelength of 488 nm in the same temperature and pressure conditions as the present studies. Refractive indices of supercritical methanol and ethanol were estimated by the Lorentz–Lorenz equation owing to the lack of a cell for high-temperature measurement. It has been, however, demonstrated that the estimation of refractive indices of supercritical alcohols by the Lorentz–Lorenz relation are confirmed to be suitable to analyze dielectric relaxation around the critical points (refs 53–55). Thus, by using these values of refractive indices, the scattering vectors were calibrated, and then the thermal diffusivities were evaluated.
- (51) Kajiya, D.; Saitow, K. Manuscript in preparation.
- (52) Kirby, C. F.; McHugh, M. A. *Rev. Sci. Instrum.* **1997**, 68, 3150.
- (53) Yao, M.; Hiejima, Y. *J. Mol. Liq.* **2002**, 96–97, 207.
- (54) Hiejima, Y.; Kajiya, Y.; Yao, M. *J. Phys.: Condens. Matter* **2001**, 13, 10307.
- (55) Hiejima, Y.; Yao, M. *J. Chem. Phys.* **2003**, 119, 7931.
- (56) Reile, E.; Jany, P.; Straub, J.; *Waerme Stoffuebertrag.* **1984**, 18, 99.
- (57) Smith, L. W.; Giglio, M.; Benedek, G. B., *Phys. Rev. Lett.* **1971**, 27, 1556.
- (58) For example: Vesovic, V.; Wakeham, W. A.; Olchoway, G. A.; Sengers, J. V.; Watson, J. T. R.; Millat, J. *J. Phys. Chem. Ref. Data* **1990**, 19, 763.
- (59) Ohmori, T.; Kimura, Y.; Hirota, N.; Terazima, M. *Phys. Chem. Chem. Phys.* **2001**, 3, 3994.
- (60) <http://pubs.acs.org/journals/jpcafh/index.html>.